ACS APPLIED MATERIALS & INTERFACES

Research Article

www.acsami.org

Alkylaminopyridine-Modified Aluminum Aminoterephthalate Metal-Organic Frameworks As Components of Reactive Self-Detoxifying Materials

Lev Bromberg,[†] Yaroslav Klichko,[†] Emily P. Chang,[†] Scott Speakman,[‡] Christine M. Straut,[§] Eugene Wilusz,[⊥] and T. Alan Hatton*,[†]

[†]Departments of Chemical Engineering and [‡]Materials Science and Engineering, Massachusetts Institute of Technology, Cambridge, Massachusetts 02139, United States

[§]Battelle Natick Operations, Natick, Massachusetts 01760, United States

[⊥]U.S. Army Natick Soldier Research, Development & Engineering Center, Materials and Defense Sciences Division, Natick, Massachusetts 01760, United States

Supporting Information

ABSTRACT: Aluminum aminoterephthalate MOF particulate materials (NH_2-MIL-101(Al) and NH_2-MIL-53(Al)), studied here as components of self-detoxifying surfaces, retained their reactivity following their covalent attachment to protective surfaces utilizing a newly developed strategy in which the MOF particles were deposited on a reactive adhesive composed of polyisobutylene/toluene diisocyanate (PIB/TDI) blends. Following MOF attachment and curing, the MOF primary amino groups were functionalized with highly nucleophilic 4-methylaminopyridine (4-MAP) by disuccinimidyl suberate-activated conjugation. The resulting MOF-4-MAP modified PIB/TDI elastomeric films were mechanically flexible and capable of degrading diisopropyl fluorophosphate (DFP), a chemical threat simulant.

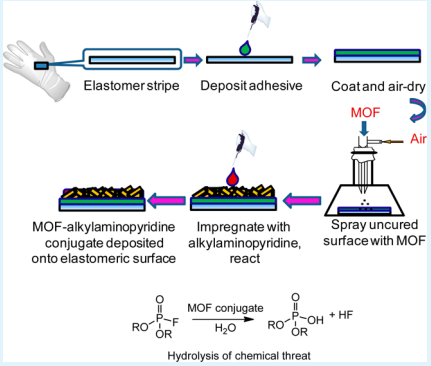

KEYWORDS: *metal organic framework, aluminum aminoterephthalate, self-detoxifying materials, alkylaminopyridine, organophosphates*

INTRODUCTION

The ability to decompose chemical threats on contact, i.e., a self-detoxifying capability, is a desirable feature of protective materials such as specialty fabrics, textiles, gloves, membranes and filters, and coatings. Incorporation of catalytic and reactive components, including organic reactive ligands, metal oxide nanocrystals, and polyoxometalates (POM), on the material's surface appears to be an established means of functionalization.[1−6]

In the present work, we devised a broadly applicable strategy for attaching functional metal−organic framework (MOF) materials to protective surfaces. MOFs possess stable crystalline structures, as well as very large porosities and surface areas, leading to outstanding sorption properties. Despite rapid progress in the search for new MOF compositions and the evaluation of their structure and properties, including capture of and reactivity toward chemical threat agents,[7−9] relatively little attention has been paid to the processing of MOF particulate materials into protective surface modifiers. Thus far, processes such as impregnation of MOFs into textile fabrics, in situ growth, electrodeposition, and electrospinning of MOF suspensions in polymeric fluids have been explored.[10−13] However, a strategy for the covalent attachment of MOF materials that enables functional MOFs to maintain their reactivity while attached to the protective material surface has not been elaborated. This paper describes a route toward covalent attachment of the MOF particles to a reactive adhesive layer deposited onto a protective material, which allows for further covalent modification of the MOFs with super-nucleophilic groups. This method produces a self-decontaminating, mechanically flexible material that is capable of degrading chemical threat agents.

Since functional organic groups can coordinate directly to the metal ions in the MOF synthesis process, the choice of such groups is not trivial. Only a few amine-functionalized frameworks are known out of the more than 10,000 MOF structures reported in the literature.[14] Two MOFs of this study are frameworks based on Al^{3+} as a nontoxic alternative to Cr^{3+}, Cu^{2+} and other metal ions commonly utilized in MOFs. Aluminum-based MOFs are readily prepared by a solvothermal route, possess appreciable thermal and chemical stability, and can be made functional by incorporating organic linkers with

Received: May 30, 2012
Accepted: August 7, 2012
Published: August 7, 2012

   dx.doi.org/10.1021/am3009696 | ACS Appl. Mater. Interfaces 2012, 4, 4595−4602

primary amines.[14] They are considered important in the fields of gas adsorption and separation of organic compounds.[15−22] To obtain an amino-functionalized MOF, 2-aminoterephthalic acid (2-ATA) is used in place of terephthalic acid as a linker molecule. Structures of the MOFs MIL-101 and MIL-53, both synthesized in this work, have been previously resolved.[15−17] Owing to the presence of amines, the NH_2-MIL-101(Al) and NH_2-MIL-53(Al) materials display basic properties and are perfect candidates for postsynthetic covalent functionalization.[14] In this study, the $-NH_2$ groups on the part of the MOF surface in contact with the adhesive layer were modified through reactions with the isocyanate groups within the adhesive, while the remaining NH_2 groups on the rest of the particle surface and within the porous structure itself were available for modification with 4-methylaminopyridine (4-MAP), a nucleophile capable of facilitating hydrolytic decomposition of an organophosphorous stimulant of chemical warfare agents. 4-MAP possesses a secondary amino group readily amenable to conjugation reactions,[23] and the 4-MAP moiety very closely resembles the structure and properties of 4-dimethylaminopyridine (DMAP), a highly efficient and industrially important organocatalyst used for a variety of organic reactions, both as a small molecule and on inorganic and polymeric supports.[24,25] DMAP has also been applied as a supernucleophilic catalyst for the esterolysis of chemical threat agents.[26]

Special care was taken to ensure that the modification processes achieved MOFs that (1) were covalently bound to the protective material, (2) bore a large payload of the covalently attached 4-MAP, and (3) possessed residual porosity that enabled sufficient access of the organophosphorous (OP) compound to the reactive 4-MAP sites. The resulting unique process and materials are described below.

EXPERIMENTAL SECTION

Materials. 2-Aminoterephthalic acid (99%, 2-ATA), aluminum chloride hexahydrate (99%), diisopropyl fluorophosphate (DFP, 99%), suberic acid bis(N-hydroxysuccinimide ester) (>95%), N,N-dimethylformamide (anhydrous, 99.9%), diisopropyl fluorophosphate (DFP, 99%), (4-methylamino)pyridine (4-MAP, 98%), N-[tris(hydroxymethyl)methyl]-2-aminoethanesulfonic acid, 2-[(2-hydroxy-1,1-bis(hydroxymethyl)ethyl)amino]ethanesulfonic acid (TES, 99%), toluene 2,4-diisocyanate (≥90%), and dibutyltin dilaurate (95%) were all obtained from Sigma-Aldrich Chemical Co. and used as received. Polyisobutylene (PIB, viscosity-average molecular weight 850,000) was obtained from Scientific Polymer Products, Inc.

Syntheses. *NH_2-MIL-101(Al).* A solution of aluminum chloride hexahydrate ($AlCl_3{\cdot}6H_2O$, 0.51 g, 2 mmol) and 2-ATA ($HOOC-C_6H_3NH_2-COOH$, 0.56 g, 3 mmol) in DMF (99.9%, 40 mL) was kept at 130 °C for 72 h in a Teflon-lined autoclave bomb. Then, the solids were separated from the solution by centrifugation (5000 *g*, 10 min) and washed with DMF under sonication for 20 min. This was followed by washing with methanol at room temperature, washing with excess hot (70 °C) methanol for 5 h, and drying under vacuum at 80 °C until constant weight was achieved. Elemental analysis, Calcd. (for unit cell, $Al_{816}C_{6528}H_{4896}N_{816}O_{4352}$): Al, 11.8; N, 6.13%; Found: Al, 12.1; C, 43.4; H, 3.52; N, 6.34%.

NH_2-MIL-53(Al). A solution of aluminum chloride hexahydrate ($AlCl_3{\cdot}6H_2O$, 99%, 2.55 g, 10 mmol) and 2-ATA (2.8 g, 15.5 mmol) in DMF (99.9%, 40 mL) was kept at 130 °C for 72 h in a Teflon-lined autoclave bomb. Then, the solids were separated from the solution by centrifugation (5000 *g*, 10 min) and washed with DMF under sonication for 20 min. This was followed by washing with methanol at room temperature, washing with excess hot (70 °C) methanol for 5 h, and drying under vacuum at 80 °C until constant weight was achieved. Elemental analysis, Calcd. (for unit cell, $Al_4C_{32}H_{24}N_4O_{20}$): Al, 12.1; N, 6.27%; Found: Al, 12.7; C, 43.8; H, 3.88; N, 6.75%.

MOF-4-MAP Conjugate (NH_2-MIL-101(Al)-4-MAP and NH_2-MIL-53(Al)-4-MAP). Dry MOF (1 g) was suspended in 10 mL of anhydrous DMF with brief sonication. A solution of 368 mg (1 mmol) suberic acid bis(N-hydroxysuccinimide ester) (disuccinimidyl suberate, or DSS) in 1 mL DMF was added and the resulting suspension was stirred at room temperature for 2 days; the solids were separated by centrifugation, washed with methanol three times and dried under vacuum. The modified MOF was mixed with 10 mL dry DMF containing 108 mg (1 mmol) of 4-methylaminopyridine, and the suspension was kept at room temperature for 2 days. The solids were separated by centrifugation, placed in excess methanol, and briefly sonicated; the solids were then again separated by centrifugation. After three washing cycles, the modified MOF was dried under vacuum and stored at −20 °C. Elemental analysis, NH_2-MIL-101(Al)-4-MAP, Calcd. (for unit cell and 1 mmol 4-MAP/g MOF): Al, 11.1; N, 6.44%; Found: Al, 11.3; N, 6.11%. For NH_2-MIL-53(Al)-4-MAP, Calcd. (for unit cell and 1 mmol 4-MAP/g MOF): Al, 11.4; N, 6.57%; Found: Al, 11.2; C, 51.1; H, 4.91; N, 6.04%.

METHODS

FTIR spectroscopy was performed with a Nicolet 8700 FTIR spectrometer (Thermo Scientific Inc.). In the transmission mode, the samples were measured in KBr. The samples were dried under vacuum to constant weight, ground and blended with KBr, and pressed to form pellets used in the measurements. Spectra were recorded over the wavenumber range between 4000 and 400 cm^{-1} at a resolution of 1 cm^{-1} and are reported as the average of 64 spectral scans. For attenuated total reflection (ATR) FTIR mode, a Golden Gate ATR accessory (Specac Ltd., Cranston, RI) was applied, with 128 scans performed at a resolution of 1 cm^{-1}. Thermogravimetric analysis (TGA) and simultaneous differential scanning calorimetry (DSC) were conducted using a Q600 TGA/DSC instrument (TA Instruments, Inc.). Samples were subjected to heating scans (20 °C/min) in a temperature ramp mode.

SEM for morphological analysis was performed using a JEOL JSM 6060 Scanning Electron Microscope. Images were collected under a 5 kV acceleration voltage at magnifications between 100x and 1000x. Samples were sputter-coated with a layer of gold using a SC7640 Sputter Coater (Quorum Technologies).

TEM was performed using a JEOL-2010 Transmission Electron Microscope at an accelerating voltage of 200 kV. Samples were prepared by placing a few drops of the MOFs dispersed in ethanol onto carbon-coated 200 mesh copper grids by Electron Microscopy Sciences.

MOF surface area and pore parameters were measured using a Micromeritics ASAP 2020 Accelerated Surface Area and Porosimetry Analyzer (Micromeritics Corp., Norcross, GA). ^1H and ^{13}C NMR spectra were collected at 25 ± 0.5 °C using a Bruker Avance-400 spectrometer operating at 400.01 and 100 MHz, respectively.

Measurement of DFP degradation on solids was performed on 20−55 mg of the MOFs or other samples.[27] The tested materials were each wet with 10 μL of water prior to the reaction. High-resolution magic angle spinning (HRMAS) ^{31}P spectroscopy was performed on a Bruker Avance-400 spectrometer operating at 161.98 MHz. Spectra were recorded with a 4-mm ^{31}P gradient probe at a temperature of 20 °C using standard Bruker software sequences. The measurement parameters were: MAS rate, 5 kHz; pulse, 90°; pulse width, 6 μs; acquisition time, 5 min. A sample weighing 10−30 mg was placed in a weighed NMR rotor (sample volume, 50 μL) and 1 or 2 μL of DFP and 1−2 μL water were applied to the top surface of the packed sample using a syringe. During each measurement, three main signals were monitored (S-1); doublets at 3.7 and 9.7 ppm coupled by the P−F bond (J_{P-F}≈970 Hz) were assigned to the reactant DFP, whereas the signal at ∼17 ppm corresponded to the degradation product (diisopropyl phosphoric acid).[27] Materials were tested in duplicate and triplicate experiments.

The kinetics of DFP degradation by hydrolysis in aqueous milieu were assessed by liquid state ^{31}P NMR spectrometry using a Bruker

Avance-400 spectrometer operating at 161.98 MHz. The reaction milieu consisted of 50 mM of TES buffer, to keep the solution pH constant at 7, and 20% (by volume) of deuterium oxide for signal locking.[28] For testing, 100 mg MOF particles were suspended in vials containing 10 mL of 80 v% TES buffer/20 v% D_2O (pH 7.0) at 10 mg/mL effective particle concentration and briefly vortexed. To the suspension, 10 μL of DFP were added via syringe and the reaction commenced. Vials were shaken at 200 rpm and 1-mL samples were withdrawn intermittently by a pipet. Each sample was immediately centrifuged (15,000*g*, 20 s) and the solids were separated. The supernatant was placed in NMR tubes and ^{31}P NMR spectra were recorded at 25 °C by the accumulation of 100 scans. The reaction time was taken to be the midpoint of the acquisition period.

The degree of DFP conversion was expressed as $F_t = \Sigma I_p/(\Sigma I_r + \Sigma I_p)$, where ΣI_r and ΣI_p are the sums of the integrations of the signals corresponding to the reactant (DFP) and the products, respectively.[27,28] The observed rate constant, k_{obs}, was found from the slope of the $\ln(1 - F_t)$ vs t plot:

$$\ln(1 - F_t) = -k_{obs}t \quad (1)$$

X-ray powder diffraction (XRD) patterns were acquired with a Panalytical X'Pert Pro multipurpose diffractometer equipped with an X'Celerator position sensitive detector coupled with a Ni β-filter and using the Cu Kα radiation. Samples were packed in a 0.1 mm-deep well on a Si zero-background plate. Programmable divergence slits were used to illuminate a constant length of the samples (8 mm), so that the constant volume assumption was preserved given that the penetration depth was calculated to be larger than the sample depth at all incident angles measured. Peak assignment and structure refinement were accomplished with X'Pert Highscore Plus v3 software. The Rietveld technique was used for structure refinement. Elemental analysis was conducted in a commercial laboratory using an ICP apparatus.

RESULTS AND DISCUSSION

The present work comprises the synthesis and characterization of functional MOF materials, MOF modification by a strongly nucleophilic moiety, with subsequent MOF attachment to elastomeric barrier films, and an evaluation of the resulting MOF-modified materials in the degradation of the chemical threat-mimicking agent, diisopropyl fluorophosphate (DFP). In the control experiments, it was found that 4-MAP possesses high reactivity toward DFP (S-2). The half-life of DFP deposited on DMAP and 4-MAP powders in the presence of water was measured to be 9 and 13 min, respectively, with the reactivity of DMAP exceeding that of 4-MAP in accordance with the higher nucleophilicity of the former.

Synthesis and Characterization of Functional MOF Materials. The amino-containing MOF material, NH_2-MIL-101(Al), was modified by the covalent attachment of 4-methylaminopyridine (4-MAP) via disuccinimidyl suberate (DSS)-activated conjugation (Figure 1).

The conjugation reaction subproduct, N-hydroxysuccinimide, is soluble in methanol and is removed by washing the functionalized MOF on a filter.

Comparison of the FTIR spectra of NH_2-MIL-101(Al)-4-MAP with those of the unmodified MOF materials indicated the presence of 4-MAP in the former. The NH_2-MIL-101(Al) MOF and its conjugate with 4-MAP were both fully soluble in 20 wt % NaOH in D_2O, enabling ^{1}H and ^{13}C NMR spectra to be obtained in this solvent (see Supporting Information, S-4 and S-5). The NMR spectra showed excellent correspondence of the assigned proton and carbon signals to the conjugate structure depicted in Figure 1. From the elemental analysis and ^{1}H NMR signal integrations, we estimated a loading of 1 mmol 4-MAP per 1 g of MOF conjugate, i.e., based on the unit cell

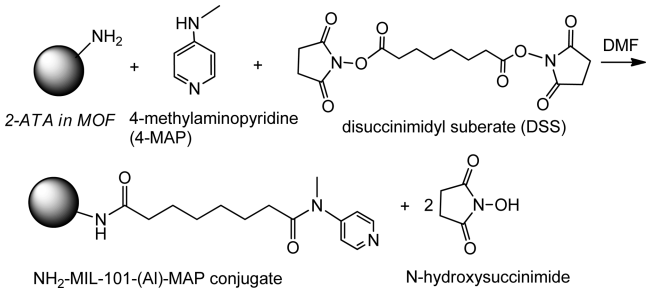

Figure 1. Reaction of 2-aminoterephthalic acid (2-ATA) and 4-methylaminopyridine (4-MAP) conjugation using DSS as an activating agent.

formula, approximately one in four amino groups present in NH_2-MIL-101(Al) were conjugated with 4-MAP.

XRD spectroscopy revealed that the preparation of the MOF by the solvothermal route in DMF resulted in two distinct species of crystalline MOF (Figure 2), depending on the initial

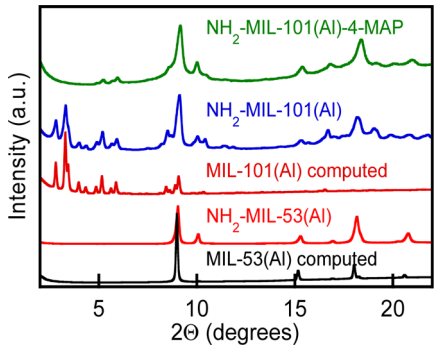

Figure 2. X-ray diffraction patterns of MIL-101(Al) and MIL-53(Al) materials, both measured and computed based on lattice parameters obtained from the Cambridge Structural Database (CSD). For computation, XRD patterns obtained from CSD for Cr-based MOF were modified by replacement of Cr with Al.

precursor ($AlCl_3.6H_2O$) concentration. The XRD spectrum of the 4-MAP modified MOF (termed NH_2-MIL-101(Al)-4-MAP conjugate) is presented in Figure 2 along with the X-ray pattern of the parent NH_2-MIL-101(Al).

The crystal structure of the species prepared with 50 mM $AlCl_3.6H_2O$ in DMF corresponded to MIL-101(Al), in accordance with the previously reported synthetic route and MOF structure.[14] The crystallographic information file used as a reference pattern, which is for MIL-101(Cr), was obtained from the Cambridge Structural Database (ref code OCUNAC). Chromium was substituted with aluminum in the reference crystal structure and the Rietveld refinement technique was used to fit the reference to the experimental pattern. Only a limited set of parameters was refined: lattice dimensions, peak width and shape, background and specimen displacement. Atomic positions were not refined. Excellent agreement between the computed MIL-101 and refined NH_2-MIL-101(Al) spectra was observed. The good agreement in peak positions implies that the synthesized material has the MIL-101 structure. The slight decrease in peak intensity and peak broadening are attributed to the presence of randomly oriented amino groups, which can occupy one of the four possible positions on the benzene ring of the p-terephthalate. Upon attachment of the 4-MAP conjugate, which gave the material an

dx.doi.org/10.1021/am3009696 | ACS Appl. Mater. Interfaces 2012, 4, 4595−4602

even more amorphous character, more significant peak broadening and peak intensity decrease were observed. However, the MIL-101 structure was not affected.

An analogous analysis was performed for NH_2-MIL-53(Al). The crystallographic information file (ref code MINVUA) obtained from the Cambridge Structure Database was used as a reference. Analysis of XRD patterns (Figure 2) indicated that with $AlCl_3.6H_2O$ concentrations greater than 250 mM, structures typical of MIL-53 were obtained. The molar ratio of aluminum chloride hexahydrate to 2-aminoterephthalic acid was set at 2:3 throughout.[14] The effect of the precursor concentration in DMF on the NH_2-MIL-53(Al) vs NH_2-MIL-101(Al) MOF synthesis has been reported previously.[29] Kapteijn and co-workers,[14,22] who were the first to report the synthesis of NH_2-MIL-101(Al) in DMF, pointed out that the MIL-101 structure is a kinetic product while MIL-53 is the thermodynamically favored structure when starting from similar synthesis compositions;[30] as a result, the MIL-53 structure is encountered with a broader variety of trivalent metals and terephthalate linkers. Owing to kinetic effects, similar synthesis concentrations can yield very different MIL structures at different reaction times. Thus, MIL-101(Fe) and MIL-53(Fe) have been synthesized after 24 and 72 h, respectively, starting from the same synthesis mixture at the same temperature.[30] Analogously, at a fixed, long reaction time (72 h) and high temperature (130 °C), a 5-fold higher precursor concentration in the present work resulted in the thermodynamically favored MIL-53(Al) material.

Based on XRD data and with the help of CrystalMaker (CrystalMaker Software, Ltd.) and SpartanModel (Wave function, Inc.) software, representations of the 3-D structures of the NH_2-MIL-101(Al) and NH_2-MIL-53(Al) MOF were prepared, as shown in Figure 3.

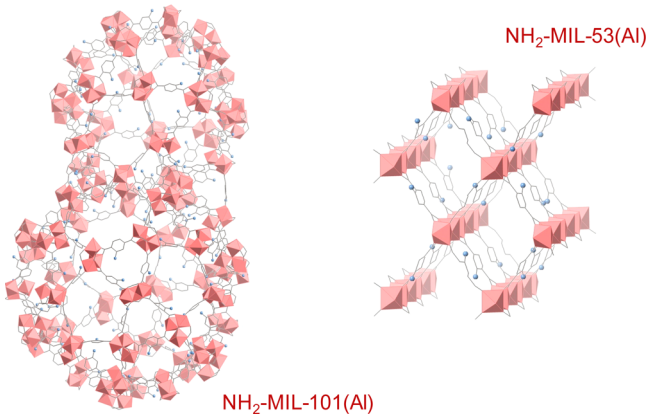

Figure 3. Structures of NH_2-MIL-101(Al) (left) showing larger and smaller spherical pores and NH_2-MIL-53(Al) (right). The inorganic cluster is represented by pink-colored octahedron, and the amino group is represented by a blue sphere.

The functional MOF materials were characterized by high resolution TEM (S-6), nitrogen adsorption isotherms at 77 K (S-7), and TGA/DSC in a nitrogen atmosphere with temperatures up to 1200 °C (Figure 4).

The specific BET surface areas for the NH_2-MIL-101(Al), NH_2-MIL-101(Al)-4-MAP, NH_2-MIL-53(Al), NH_2-MIL-53(Al)-4-MAP samples were 2600, 1590, 930, and 660 m^2/g, respectively. The values obtained for NH_2-MIL-101(Al) and NH_2-MIL-53(Al) are considerably higher than those reported

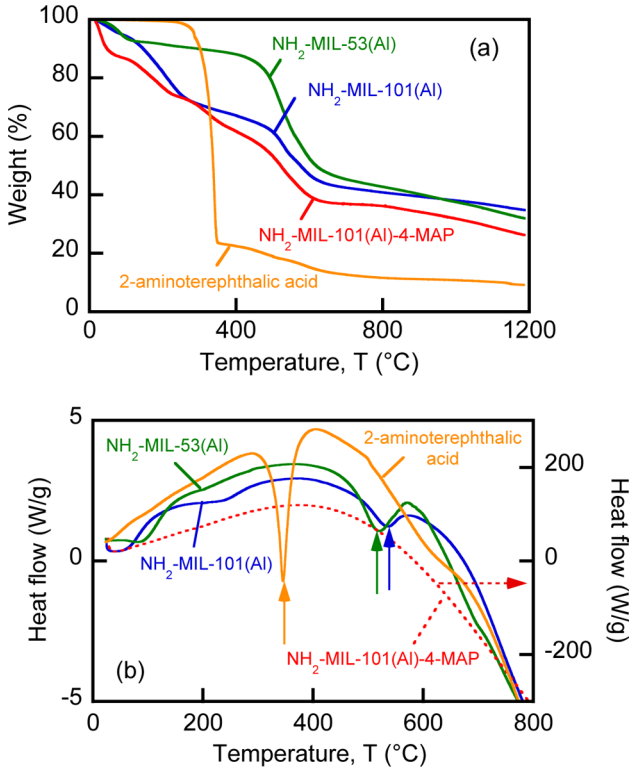

Figure 4. (a) Thermogravimetric analysis of NH_2-MIL-51(Al), NH_2-MIL-101(Al), NH_2-MIL-101(Al)-4-MAP and 2-aminoterephthalic acid in a nitrogen atmosphere. Heating scan, 20 °C/min. (b) Differential scanning calorimetry (DSC) thermograms of NH_2-MIL-101(Al), NH_2-MIL-53(Al), NH_2-MIL-101(Al)-4-MAP and 2-aminoterephthalic acid in a nitrogen atmosphere. Heating scan, 20 °C/min. Solid arrows indicate endothermic melting peaks of 2-aminoterephthalic acid, NH_2-MIL-53(Al) and NH_2-MIL-101(Al). The dotted arrow indicates that the heat flow values for NH_2-MIL-101(Al)-4-MAP are shown by the vertical heat flow axis on the right.

previously (2100 and 675 m^2/g, respectively),[14,22] which is probably due to the more extensive washing steps used in the present work than in the earlier studies. The BET surface area of the MOF modified by 4-MAP was 1.4- to 1.6-fold lower than that of the unmodified MOF due to the partial filling of the pores by the organic 4-MAP molecules. This pore-filling effect is much less pronounced than with bulkier molecules such as phosphotungstic acid (PTA), which reduces the BET surface area of MIL-101 4- to 5-fold when it is introduced to the MOF pores.[31]

Thermogravimetric analysis (TGA/DSC) of NH_2-MIL-101(Al), its conjugate with 4-MAP, NH_2-MIL-53(Al) and 2-aminotherephthalic acid in nitrogen is shown in Figure 4. The MOF samples and the 4-MAP MOF conjugate released up to 6 and 13 wt %, respectively, of solvent at temperatures <100 °C. The MOF materials decomposed only at temperatures above 450 °C, thus demonstrating remarkable thermal stability. A similar degradation of NH_2-MIL-53(Al) detected by TGA in the 450−500 °C range has been reported previously.[21] The MOF-4-MAP conjugate lost approximately 28% of its weight in the range 105−450 °C due to degradation of organic molecules other than 2-ATA. It is interesting to observe that the MOF materials were more stable than 2-ATA alone. The latter exhibited endothermic melting and decomposition starting at 263 °C and ending at 360 °C, with the endotherm centered at 345 °C at the given scan rate. This result corresponds well with

the published data on the 2-ATA melting/decomposition temperature measured at a ramp rate of 10 °C/min.[32] The melting point of 2-ATA was measured to be 325 °C by a capillary melting apparatus. The observed 150−170 °C differences in the MOF melting/degradation compared to those of 2-ATA are due to stabilization via complexation of the linker (2-ATA) with aluminum (Figure 4).

Self-Detoxifying Elastomeric Films. The covalent attachment of amino-functional MOFs required the selection of an adhesive to be deposited on the surface of the protective materials. We chose a high-molecular weight polyisobutylene (PIB) to be a component of the adhesive because of its tackiness, mechanical flexibility, low cohesive strength and nonirritating nature,[33,34] with the last property being important if the adhesive is required to contact human skin. Toluene diisocyanate (TDI) was chosen as a reactive component of the curable adhesive. TDI is fully miscible with PIB in toluene; the PIB-TDI blends were stable at room temperature in a water-free atmosphere for at least 3 days without discernible gelation. Highly viscous, 10 wt %, solutions of PIB in toluene containing 5 wt % of TDI and 0.01 wt % dibutyltin dilaurate (reaction catalyst) were selected as they did not wick into the pores of the MOF, but did react on the surfaces of the MOF particles with the 2-ATA component (Figure 5). TDI is capable of

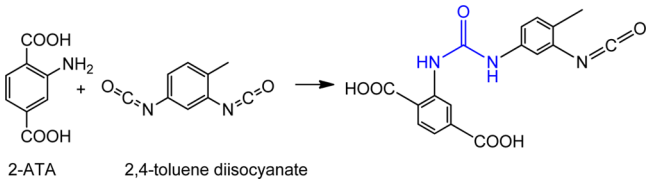

Figure 5. Reaction between 2-aminoterephthalic acid (2-ATA) and 2,4-toluene diisocyanate (TDI). Carboxyl groups of 2-ATA chelated to Al^{3+} in the MOF and were not reactive with isocyanate.

reacting with amines present in our MOF as well as with hydroxyls present on cotton, wool, wood, a variety of fabrics, and metal oxide surfaces. The process of attachment of the MOF particles to the surface of a butyl rubber glove, followed by the MOF functionalization, is shown schematically in Figure 6. MOF particles were attached by spraying them onto an evenly coated, uncured, tacky PIB/TID layer on the rubber surface. The particles attached to the rubber surface were impregnated with 4-MAP/DSS (1:1 mol/mol) solution in DMF and were allowed to react at room temperature for 48 h and at 70 °C for 3 h, after which the reaction products and DMF were washed off the MOF-coated rubber by methanol and the surface was dried by a stream of air. After curing, the particles were bound firmly to the rubber surface, without flaking even after repeated 50% elongation of the rubber.

SEM images taken at the end of the process show complete coverage of the rubber by multiple layers of the MOF particles (Figure 7). The adhesion of the cured PIB/TDI films, with or without MOF, on the butyl rubber of the glove surface was so strong that the mechanical separation of the deposited films from the glove was not possible. However, a composite film formed by the deposition of PIB/TDI on high-density Teflon, which was subsequently coated with MOFs and then treated to form the MOF-4-MAP conjugates, could be detached from the substrate and subjected to TGA analysis (S-8). Although the film was completely covered by the MOF layers, the MOF only

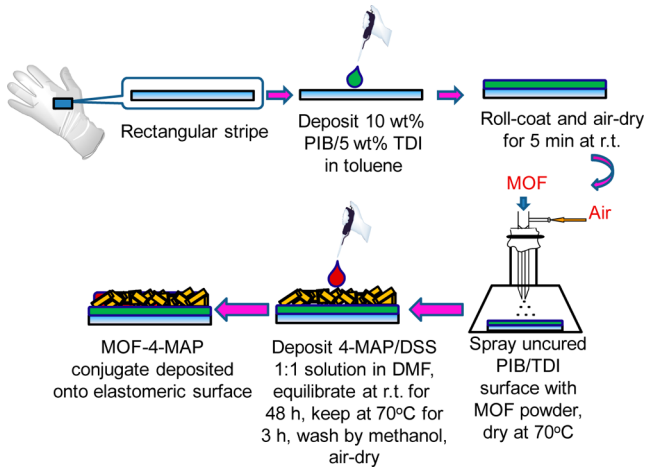

Figure 6. Schematic depicting the process of synthesis of elastomeric films deposited onto the outer surfaces of the Guardian butyl rubber gloves (Guardian Manufacturing Company, Willard, OH) modified with MOFs that are further functionalized by the covalent attachment of 4-MAP.

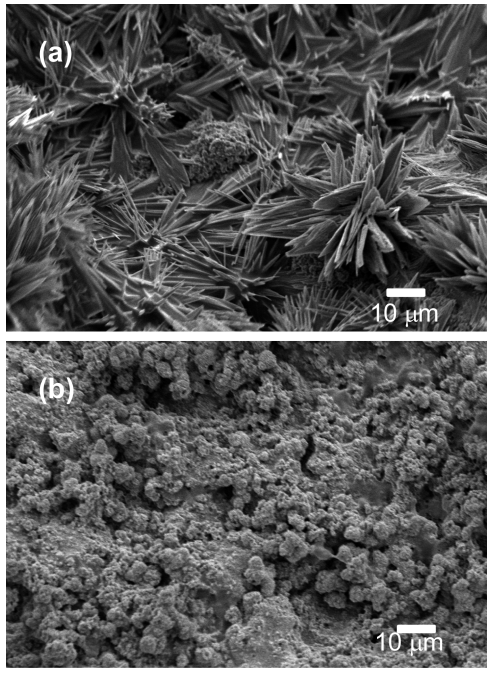

Figure 7. SEM images of (a) NH_2-MIL-53(Al)-4-MAP and (b) NH_2-MIL-101(Al)-4-MAP particle layers deposited onto elastomeric film via the processes depicted in Figure 6.

contributed to 5−7% of the composite's total weight because the MOF particle layer has a low density.

The reactions occurring during the processes in Figure 6 were observed by ATR-FTIR (Figure 8). The band at 2257 cm^{-1}, which is characteristic of the isocyanate groups of TDI, appears on the glove surface upon the PIB/TDI film deposition, becomes less intense with partial reaction of the isocyanate with the amine groups of the MOF, and disappears with the complete curing of the film-MOF composite. The appearance of 4-MAP is discernible by the band at 1188 cm^{-1} corresponding to the C−N stretching of the 4-methylamino-pyridine ring.

dx.doi.org/10.1021/am3009696 | ACS Appl. Mater. Interfaces 2012, 4, 4595−4602

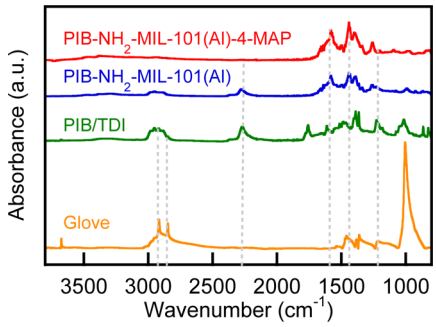

Figure 8. Attenuated total reflectance (ATR) FTIR spectra of a Guardian™ butyl rubber glove during different steps of the process shown in Figure 6, including: the untreated butyl rubber glove, uncured polyisobutylene/2,4-toluene diisocyanate (PIB/TDI) film deposited onto the glove, NH_2-MIL-101(Al) material deposited onto the PIB/TDI film and partially reacted, and NH_2-MIL-101(Al) material conjugated with 4-MAP ligand on the surface of the PIB/TDI film deposited onto the glove surface (designated PIB-NH_2-MIL-101(Al)-4-MAP).

Vertical lines at 2915, 2847, 2257, 1573, and 1188 cm^{-1} show bands corresponding to symmetric CH_3 stretching of 1,4-polyisoprene, symmetric CH_2 stretching of 1,4-polyisoprene, stretching of N═C═O, stretching vibration of the aluminum carboxylates in MOF, and C−N stretching of the 4-methylaminopyridine ring, respectively.

Performance of the MOF and MOF-Modified Elastomeric Films in DFP Degradation. Hydrolytic decomposition of diisopropyl fluorophosphate (DFP), a close analogue of 2-(fluoromethylphosphoryl)oxypropane (sarin, a chemical warfare agent) is a widely tested reaction for evaluating the performance of materials designed for the degradation of the organophosphorous chemical threat agents.[27,35,36] Degradation of DFP (Figure 9) is mediated by nucleophilic groups through the nucleophilic attack on the pentavalent phosphorus of DFP, resulting in P−F bond cleavage and fluorine release.

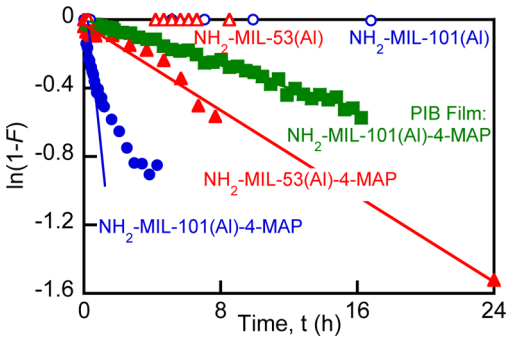

Figure 9. Typical kinetics of DFP degradation by NH_2-MIL-101(Al)-4-MAP, NH_2-MIL-53(Al)-4-MAP, PIB/TDI film covalently modified by attachment of NH_2-MIL-101(Al) conjugated with 4-MAP, and by NH_2-MIL-101(Al) and NH_2-MIL-53(Al) samples without the 4-MAP. *F* denotes the degree of conversion measured using ^{31}P HRMAS NMR, as described in the Experimental Section.

Degradation of DFP was tested via deposition of DFP liquid directly onto materials prewet with water, at water/DFP mol/mol ratios ranging from 5 to 15. This amount of water was required to enable transport of DFP, to and within the MOFs, and dissociation of the complexes of the product (diisopropyl phosphoric acid) with the basic and nucleophilic binding sites of the 4-MAP and/or $-NH_2$ groups of the MOF. PIB/TDI films modified with 4-MAP and MOF layers were prepared as depicted in Figure 6, but without the protective glove. The PIB/TDI solution was first cast onto the Teflon surface, then modified and cured as in Figure 6; the resulting films were carefully detached from Teflon with a scalpel. Care was taken to pack the films into the NMR rotor with the MOF layers exposed outward for accessibility to DFP and water. Kinetic decomposition studies (Figure 9) demonstrated that NH_2-MIL-101(Al) and NH_2-MIL-53(Al) MOFs were unreactive toward DFP, even in the presence of added water. Given that amines can, in general, decompose OPs via base-catalyzed hydrolysis,[37,38] we can conclude that reactivity of 2-ATA incorporated within the MOF was insufficient for the reaction to occur. However, modification of the MOF by 4-MAP dramatically enhanced the reaction rate, with the observed rate constants (k_{obs}, see eqn1) of the initial DFP degradation measured to be in the 0.064 to 0.75 h^{-1} range, depending on the actual amount of solid sample loaded. The corresponding DFP half-life values ranged from 0.9 to 10 h, consistent with the 0.8−5 h reported previously for analogous experiments with montmorillonite K-10 functionalized with sodium pralidoximate by intercalation.[27] However, due to the possibility of their covalent attachment to solid surfaces, the MOFs presented herein are advantageous over intercalated clays as components of self-detoxifying materials.

The degradation was typically biphasic with 4-MAP-modified MOF and accelerated with a larger amount of solid sample loaded into the NMR rotor, as expected. The biphasic nature of the degradation kinetics with NH_2-MIL-101(Al)-4-MAP was probably due to the adsorptive nature of the MOF and heterogeneity of the tested DFP-particle system. The DFP droplet deposited onto the MOF layer started degrading rapidly with the 4-MAP moieties available in the immediate proximity, but then the kinetics became transport-limited and slowed down several-fold, due to the need for DFP to permeate through the particle toward unreacted 4-MAP sites. The strongly basic 4-MAP can form a salt-like complex with the reaction products, hydrofluoric and diisopropylphosphoric acids, which would render the 4-MAP group unavailable for further reaction without dissociation in the absence of a sufficient amount of water. Under these conditions, the 4-MAP conjugate is a reactant that does not participate in any catalytic turnover. Due to the transport limitations, within a 24 h period, only 50 to 80% of the initial DFP was degraded on 4-MAP-modified MOF particles. Approximately 55% of the initial DFP was degraded on the elastomeric film modified with NH_2-MIL-101(Al)-4-MAP layers.

Although we do not foresee a repeated utilization of the presented MOF-modified protective surfaces after their contact with chemical threat agents, we were interested in addressing the question as to whether the alkylaminopyridine-modified MOF particles by themselves could be reused after being washed with water under mild conditions (neutral pH, ambient temperature, no bleach agents). The kinetics of DFP degradation in aqueous suspensions of NH_2-MIL-101(Al)-4-MAP at room temperature were observed for three consecutive cycles of use. After each cycle, the MOF particles were separated from the suspension by centrifugation, rinsed with deionized water and dried under vacuum. The results are shown in Figure 10. In the absence of transport limitations and the effects of 4-MAP sites poisoning, the hydrolysis of DFP with NH_2-MIL-101(Al)-4-MAP was a linear, first-order

dx.doi.org/10.1021/am3009696 | ACS Appl. Mater. Interfaces 2012, 4, 4595−4602

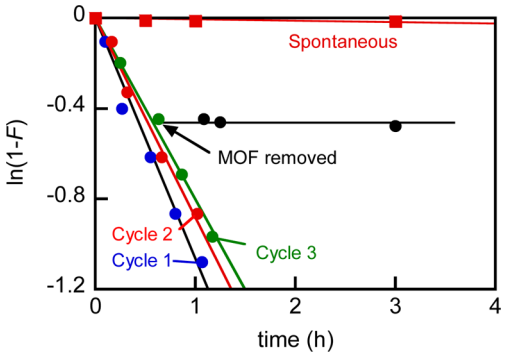

Figure 10. Kinetics of DFP degradation in aqueous suspensions of NH_2-MIL-101(Al)-4-MAP particles at pH 7.0 and T = 25 °C repeated in three consecutive cycles. After each cycle, the MOF particles were separated from the suspension by centrifugation, rinsed by deionized water and dried under vacuum. Spontaneous DFP hydrolysis without any MOF at pH 7.0 is shown along with the hydrolysis measured in the reaction medium (Cycle 3) after separating MOF particles. The moment of particle separation is shown by an arrow. Initial particle concentration in each cycle, 10 mg/mL.

reaction (R^2 > 0.98 in all cases) that went to 98−100% DFP conversion in less than 3 h. The observed rate constants yielded DFP half-life values of 0.65, 0.87, and 0.87 h in cycles 1, 2, and 3, respectively. These results indicate that the NH_2-MIL-101(Al)-4-MAP particles were sufficiently stable over three cycles and, within the experimental error, yielded repeatable, *catalytic* hydrolysis of DFP. The second-order reaction rate in these reactions was estimated to be $(1-3)x10^{-2}$ $M^{-1}s^{-1}$, assuming full accessibility of the 4-MAP catalytic sites present in the suspensions at 10 mM concentration. This estimate is at least 10-fold higher than the second-order reaction rate, obtained under identical conditions,[28] in solutions of α-nucleophilic hydroxamic acids such as isonicotinhydroxamic acid methiodide. Spontaneous hydrolysis in the absence of MOF was at least 100 times slower than the catalyzed reaction.

Of note, the leaching of 4-MAP attached to the MOF was minimal, as indicated by the absence of any discernible reaction in the medium that was separated from the NH_2-MIL-101(Al)-4-MAP particles. Analogously, no DFP hydrolysis was observed within 3 h when 10 μL of DFP were added to wash-outs from a film coated with NH_2-MIL-101(Al)-4-MAP. Specifically, a PIB/TDI film coated with NH_2-MIL-101(Al)-4-MAP (124 mg total) was immersed in 2 mL of the TES buffer/D_2O (pH 7.0) and shaken for 1 h. Then the film was removed and the aqueous wash-out was mixed with DFP and the DFP hydrolysis was measured by liquid-state ^{31}P NMR. The results indicate that the 4-MAP covalent attachment onto the MOF particles and to the PIB/TDI films remained intact, so that no hydrolysis occurred that would be catalyzed by the leached 4-MAP. In turn, one can classify NH_2-MIL-101(Al)-4-MAP particles to be a *heterogeneous catalyst* for the DFP hydrolysis.

CONCLUDING REMARKS

MOF materials possess high surface area, open pores and sufficient thermal, chemical and mechanical stability to become carriers of functional components in a variety of devices. However, methods of MOF layer deposition enabling one to maintain MOF functionality are still lacking. This work demonstrated a novel approach toward creating self-detoxifying materials via the covalent attachment of amino-functional, aluminum-based MOF particles to reactive adhesives, which themselves can be deposited onto a variety of surfaces. The attached MOF is further covalently modified with a highly nucleophilic alkylaminopyridine moiety such as 4-MAP. We envision that the primary amino groups of the attached MOF can also be conjugated with other functional molecules, including OP chemical threat-degrading enzymes,[39] organometallic catalysts,[40] reactive polymers[41] or polyoxometalates,[42] thus producing efficient self-detoxifying materials.

ASSOCIATED CONTENT

Supporting Information

^{31}P NMR spectra, DFP degradation kinetics, FTIR, ^{1}H and ^{13}C NMR spectra of MOF materials, high-resolution TEM images, BET nitrogen adsorption isotherms, TGA thermograms. This material is available free of charge via the Internet at http://pubs.acs.org/.

AUTHOR INFORMATION

Corresponding Author

*E-mail: tahatton@mit.edu.

Notes

The authors declare no competing financial interest.

ACKNOWLEDGMENTS

The authors were supported by the Defense Threat Reduction Agency, in part by Grant HDTRA1-09-1-0012, and by the U.S. Army Research Office.

REFERENCES

(1) Gall, R. D.; Hill, C. L.; Walker, J. E. *J. Catal.* **1996**, *159*, 473−478.
(2) Schreuder-Gibson, H.; Gibson, P.; Seneca, K.; Sennett, M.; Walker, J.; Yeomans, W.; Ziegler, D.; Tsai, P. P. *J. Adv. Mater.* **2002**, *34*, 44−55.
(3) Wu, K. H.; Yu, P. Y.; Yang, C. C.; Wang, G. P.; Chao, C. M. *Polym. Degrad. Stab.* **2009**, *94*, 1411−1418.
(4) Ramkumar, S. S.; Sata, U.; Hussain, M. *Advances in Biological and Chemical Terrorism Countermeasures*; Kendall, R. J., Presley, S. M., Austin, G. P., Smith, P. N., Eds; CRC Press: Boca Raton, FL, 2008, Chapter 8; pp 203−227.
(5) Hill, C. L.; Okun, N. M.; Hillesheim, D. A.; Geletii, Y. V. In: *Anti-Terrorism and Homeland Defense: Polymers and Materials*;Reynolds, J. G., Lawson, G. E.,Koester, C. J., Eds.; ACS Symposium Series 980; American Chemical Society: Washington, D.C., 2007; Chapter 12, p 198.
(6) Ochanda, F. O.; Furukawa, H.; Yaghi, O. M.; Hinestroza, J. P. *243rd ACS National Meeting & Exposition*; San Diego, CA, March 25−29, 2012 ; American Chemical Society: Washington, D.C., 2012.
(7) Britt, D.; Tranchemontagne, D.; Yaghi, O. M. *Proc. Natl. Acad. Sci. U.S.A.* **2008**, *105*, 11623−11627.
(8) Montoro, C.; Linares, F.; Procopio, E. Q.; Senkovska, I.; Kaskel, S.; Galli, S.; Masciocchi, N.; Barea, E.; Navarro, J. A. R. *J. Am. Chem. Soc.* **2011**, *133*, 11888−11891.
(9) Song, J.; Luo, Z.; Britt, D. K.; Furukawa, H.; Yaghi, O. M.; Hardcastle, K. I.; Hill, C. L. *J. Am. Chem. Soc.* **2011**, *133*, 16839−16846.
(10) Kusgens, P.; Siegle, S.; Kaskel, S. *Adv. Eng. Mater.* **2009**, *11*, 93−95.
(11) Centrone, A.; Yang, Y.; Speakman, S.; Bromberg, L.; Rutledge, G. C.; Hatton, T. A. *J. Am. Chem. Soc.* **2010**, *132*, 15687−15691.
(12) Rose, M.; Böhringer, B.; Jolly, M.; Fischer, R.; Kaskel, S. *Adv. Eng. Mater.* **2011**, *13*, 356−360.
(13) Li, M.; Dincă, M. *J. Am. Chem. Soc.* **2011**, *133*, 12926−12929.
(14) Serra-Crespo, P.; Ramos-Fernandez, E. V.; Gascon, J.; F., Kapteijn, F. *Chem. Mater.* **2011**, *23*, 2565−2572.

(15) Loiseau, T.; Serre, C.; Huguenard, C.; Fink, G.; Taulelle, F.; Henry, M.; Bataille, T.; Férey, G. *Chem.—Eur. J.* **2004**, *10*, 1373−1382.
(16) Ahnfeldt, T.; Guillou, N.; Gunzelmann, D.; Margiolaki, I.; Loiseau, T.; Ferey, G.; Senker, J.; Stock, N. *Angew. Chem., Int. Ed.* **2009**, *48*, 5163−5166.
(17) Haque, E.; Khan, N. A.; Kim, C. M.; Jhung, S. H. *Cryst. Growth Des.* **2011**, *11*, 4413−4421.
(18) Alaerts, L.; Maes, M.; Giebeler, L.; Jacobs, P. A.; Martens, J. A.; Denayer, J. F. M.; Kirschhock, C. E. A.; De Vos, D. E. *J. Am. Chem. Soc.* **2008**, *130*, 14170−14170.
(19) Stavitski, E.; Pidko, E. A.; Couck, S.; Remy, T.; Hensen, E. J. M.; Weckhuysen, B. M.; Denayer, J.; Gascon, J.; Kapteijn, F. *Langmuir* **2011**, *27*, 3970−3976.
(20) Juan-Alcañiz, J.; Gascon, J.; Kapteijn, F. *J. Mater. Chem.* **2012**, *22*, 10102−10118.
(21) Couck, S.; Denayer, J. F. M.; Baron, G. V.; Remy, T.; Gascon, J.; Kapteijn, F. *J. Am. Chem. Soc.* **2009**, *131*, 6326−6327.
(22) Gascon, J.; Aktay, U.; Hernandez-Alonso, M. D.; van Klink, G. P. M.; Kapteijn, F. *J. Catal.* **2009**, *261*, 75−87.
(23) Pulko, I.; Wall, J.; Krajnc, P.; Cameron, N. R. *Chem. Eur. J.* **2010**, *16*, 2350−2354.
(24) Ragnarsson, U.; Grehn, L. *Acc. Chem. Res.* **1998**, *31*, 494−501.
(25) Price, K. E.; Mason, B. P.; Bogdan, A. R.; Broadwater, S. J.; Steinbacher, J. L.; McQuade, D. T. *J. Am. Chem. Soc.* **2006**, *128*, 10376−10377.
(26) Yokley, E. M.; Nielsen, R. B. Hypernucleophilic Catalysts For Detoxification Of Chemical Threat Agents. U.S. Patent Application 20110028774, Publication date: 02/03/2011.
(27) Bromberg, L.; Straut, C. M.; Centrone, A.; Wilusz, E.; Hatton, T. A. *ACS Appl. Mater. & Interfaces* **2011**, *3*, 1479−1484.
(28) Chen, L.; Bromberg, L.; Lee, J. A.; Zhang, H.; Schreuder-Gibson, H.; Gibson, P.; Walker, J.; Hammond, P. T.; Hatton, T. A.; Rutledge, G. C. *Chem. Mater.* **2010**, *22*, 1429−1436.
(29) Stavitski, E.; Goesten, M.; Juan-Alcaniz, J.; Martinez-Joaristi, A.; Serra-Crespo, P.; Petukhov, A. V.; Gascon, J.; Kapteijn, F. *Angew. Chem., Int. Ed.* **2011**, *50*, 9624−9628.
(30) Bauer, S.; Serre, C.; Devic, T.; Horcajada, P.; Marrot, J.; Ferey, G.; Stock, N. *Inorg. Chem.* **2008**, *47*, 7568−7576.
(31) Bromberg, L.; Diao, Y.; Wu, H.; Speakman, S. A.; Hatton, T. A. *Chem. Mater.* **2012**, *24*, 1664−1675.
(32) Arias-Pardilla, J.; Salavagione, H. J.; Barbero, C.; Morallón, E.; Vázquez, J. L. *Eur. Polym. J.* **2006**, *42*, 1521−1532.
(33) Willenbacher, N.; Lebedeva, O. V. In *Technology of Pressure-Sensitive Adhesives and Products*,; Benedek, I., Feldstein, M. M., Eds.; CRC Press: Boca Raton, FL, 2009; Chapter 4.
(34) Martin-Martinez, J. M. In *The Mechanics of Adhesion*; Dillard, D. A., Pocius, A. V., Eds.; Elsevier: Amsterdam, 2002; Chapter 13, pp 573−675.
(35) Bromberg, L.; Hatton, T. A. *Ind. Eng. Chem. Res.* **2005**, *44*, 7991−7998.
(36) Bromberg, L.; Hatton, T. A. *Ind. Eng. Chem. Res.* **2007**, *46*, 3296−3303.
(37) Wagner-Jauregg, T.; O'Neill, J. J.; Summerson, W. J. *J. Am. Chem. Soc.* **1951**, *73*, 5202−5206.
(38) Epstein, J.; Cannon, P. L.; Sowa, J. R. *J. Am. Chem. Soc.* **1970**, *92*, 7390−7393.
(39) McDaniel, C. S.; McDaniel, J.; Wales, M. E.; Wild, J. R. *Prog. Org. Coatings* **2006**, *55*, 182−188.
(40) Corma, A.; García, H. *Chem. Rev.* **2002**, *102*, 3837−3892.
(41) Bromberg, L.; Schreuder-Gibson, H.; Creasy, W. R.; McGarvey, D. J.; Fry, R. A.; Hatton, T. A. *Ind. Eng. Chem. Res.* **2009**, *48*, 1650−1659.
(42) Duffort, V.; Thouvenot, R.; Afonso, C.; Izzet, G.; Proust, A. *Chem. Commun.* **2009**, 6062−6064.